Electronic Supplemental Information

Distant ultrafast energy-transfer in a trimetallic {Ru-Ru-Cr} complex facilitated by hole delocalization

Alejandro Cadranel, Jaired Tate, Paola S. Oviedo, Shiori Yamazaki, José H. Hodak, Luis M. Baraldo , and Valeria D. Kleiman

Figure S1: ^{1}H NMR spectrum of **2** in acetone-d_6. Signals are assigned as described in the text.

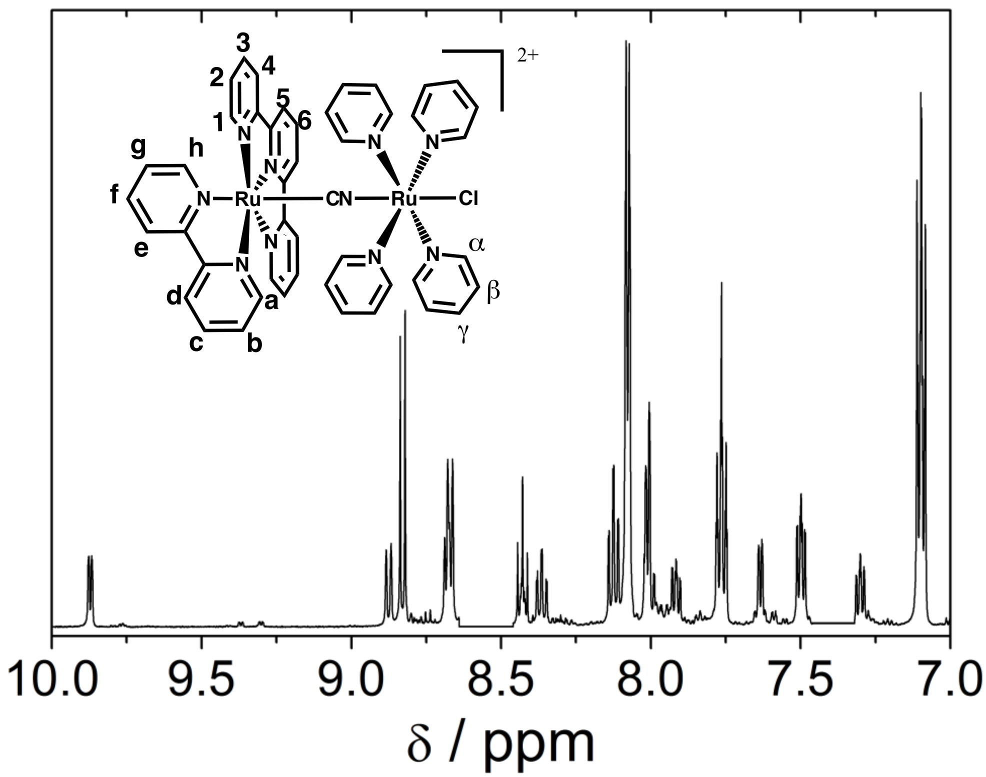

Table S1. Selected distances and angles of the crystallographic structures of **1**, **2**, and **3**. Data for **1** is taken from reference [1]

1	**2**	**3**	**1**	**2**	**3**
Distances / Å			Angles / °		
Ru$_{tb}$-N$_{tpy}$			**N-Ru$_{tb}$-N$_{tpy}$**		
1.966(2) 2.060(2) 2.078(2)	1.951(8) 2.082(9) 2.087(8)	1.958(8) 2.075(10) 2.094(10)	79.23(10) 79.33(9)	79.0(4) 79.4(3)	78.8(4) 79.5(4)
Ru$_{tb}$-N$_{bpy}$			**N-Ru$_{tb}$-N$_{bpy}$**		
2.049(2) 2.076(2)	2.093(9) 2.122(10)	2.078(8) 2.086(9)	78.52(8)	77.1(4)	78.4(4)
Ru$_{py}$-N$_{py}$					
- - - -	2.085(11) 2.098(10) 2.102(12) 2.112(13)	2.076(10) 2.077(10) 2.100(9) 2.112(9)			
Ru$_{tb}$-C$_{bridge}$			**Ru$_{tb}$-C-N$_{bridge}$**		
-	1.970(12)	2.007(12)	-	176.9(9)	174.3(11)
C-N$_{bridge}$			**C-N$_{bridge}$-Ru$_{py}$**		
-	1.163(14)	1.123(13)	-	175.2(9)	176.6(10)
N$_{bridge}$-Ru$_{py}$			**N$_{bridge}$-Ru-N$_{bridge}$**		
-	2.028(10)	2.030(8)	-	-	176.9(4)
Ru$_{tb}$-Ru$_{py}$			**Ru$_{tb}$-N-C$_{bridge}$**		
-	5.155	5.148	170.1(2)	-	167.8(11)
Ru-N$_{bridge}$			**N-C$_{bridge}$-Cr**		
2.037(2)	-	2.020(9)	173.8(3)	-	174.8(11)
N-C$_{bridge}$			**Ru$_{tb}$-Ru$_{py}$-Cr**		
1.144(3)	-	1.177(15)	-	-	164.8
Ru$_{tb}$-Cr					
5.218	-	10.279			

Table S2. Crystallographic data of **2** and **3**. CCDC 1505901 and 1023002 contains the supplementary crystallographic data for **2** and **3** respectively. These data can be obtained free of charge from the Cambridge Crystallographic Data Center via www.ccdc.cam.ac.uk/data_request/cif.

Empirical Formula	**C_{47} H_{43} Cl F_{12} N_{10} O P_2 Ru_2**	**C_{54} H_{45} Cr N_{16} O_8 Ru_2 S**
Formula weight	1291.44	1332.26
***T* (K)**	298 (2)	298 (2)
Crystal system	Monoclinic	Monoclinic
Space Group	$P2_1/c$	$P2_1$
***a* (Å)**	13.779(3)	12.3182(17)
***b* (Å)**	18.119(4)	22.004(2)
***c* (Å)**	22.414(4)	13.2118(17)
β(°)	92.599(15)	109.093(14)
V (Å^3)	5590(2)	3384.0(6)
Z	4	2
D_{calc} (mg/m^3)	1.534	1.307
Absorption coefficient (mm^{-1})	0.729	0.686
***F*(000)**	2584	1346
Crystal size (mm)	0.06 x 0.18 x 0.48	0.03 x 0.40 x 0.45
Crystal color/shape	dark red/ plate	red/ plate
Radiation, graphite monochr.	MoKα, λ= 0.71069 Å	MoKα, λ = 0.71069 Å
θ Range data collection (°)	3.58-29.11	3.62– 27.00
Index ranges	$-12 \leq h \leq 17$	$-14 \leq h \leq 15$
	$-22 \leq k \leq 22$	$-28 \leq k \leq 24$
	$-28 \leq l \leq 28$	$-16 \leq l \leq 16$
Reflections collected/unique	27324/11547 (Rint= 0.1715)	18321/ 11793 (Rint= 0.0949)
Observed reflections [I>2σ(I)]	5155	8209
Completeness (%)	0.996	0.80
Maximum / minimum transmission	1.000 / 0.45450	1.000 / 0.72899
Refinement method	full-matrix least-squares on F^2	full-matrix least-squares on F^2
Weights, *w*	$1/[\sigma^2(F_o^2)+(0.1669P)^2+0.0000P]$ where $P=(Fo^2+2F_c^2)/3$	$1/[\sigma^2(F_o^2)+(0.1273P)^2+0.0000P]$ where $P=(Fo^2+2F_c^2)/3$
Data/restraints/parameters	11547/8/676	11793/1/742
Goodness-of-fit (GOF) on F^2	1.017	1.059
Final R-index [I>2σ(I)]/ all data	0.1127/0.2005	0.0874/ 0.1142
***w*R index [I>2σ(I)] /all data**	0.2734/0.3624	0.2135/0.2583
Largest peak and hole (e A^{-3})	1.503 and -0.843	2.154 and -0.936

Table S3 - Electrochemical data for complexes **1**, **2** and **3**. a) Irreversible, cathodic peak. Data for **1** is taken from ref.[1]

Comp.	**Solvent**	$E_{1/2}$ (ΔE_p)/V (mV)				
		Ru_{pp}(III/II)	Ru_{py}(III/II)	tpy(0/-)	bpy(0/-)	Cr(III/II)
1	ACN	1.10 (190)	-	-1.28 (120)	-1.60 (130)	-1.83 [a]
2	ACN	1.60 (80)	0.73 (80)	-1.17 (120)	-1.54 (200)	-
3	DMSO/H_2O	1.64 (nd)	1.05 (nd)	-1.13 (nd)	-1.49 (nd)	nd

Table S4: Assignment of IR absorption bands.

Complex	ν_{CN} / cm^{-1}	Assignment
1	2119	terminal
2	2096	bridge
3	2127 2120(sh) 2104	terminal bridge bridge

Table S5 - UV-vis

Comp.	**Solvent**	**UV-Vis abs.**	
		λ_{MLCT} / nm(ε / $10^3 M^{-1} cm^{-1}$)	
		π^*(py)←dπ(Ru)	π^*(pp)←dπ(Ru)
1[1]	DMSO	-	353 (5.5) (sh) 478 (8.9)
2	DMSO	380 (19.1)	440 (10.3) (sh)
3	DMSO	368 (20.0)	450 (7.0)

Figure S3: Emission lifetimes measured in DMSO. The fits correspond to monoexponential decays.

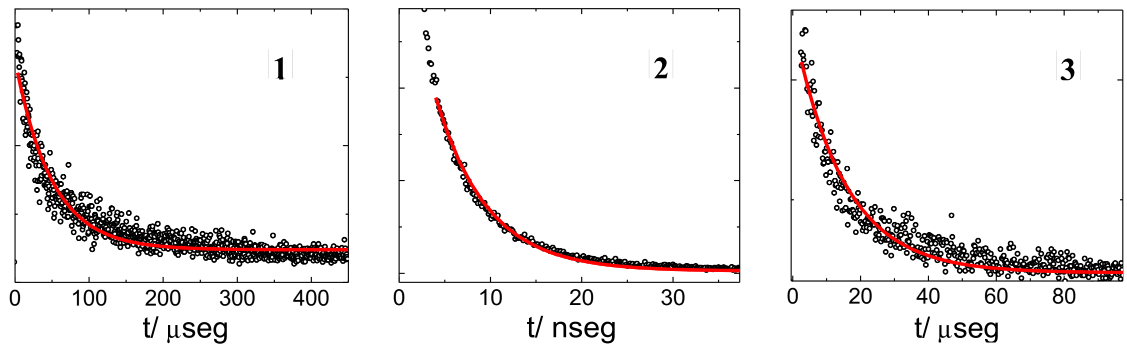

$\tau_1 = 49 \mu sec$ $\tau_2 = 5.6 nsec$ $\tau_3 = 15\ \mu sec$

Figure S4: Broadband Transient absorption spectra of compounds **2** (top) and **3** (bottom) in DMSO upon excitation at 400 nm leading to π*(py) ←t_{2g}(Ru) absorption. The spectra shown correspond to negative times (—), 1 ps (—), 5 -for **2**- and14 ps -for **3**- (—), 25 -for **2**- and 50 ps -for **3**- (—), and 240 -for **2**- and 300 ps -for **3**- (—). The gap (380- 420 nm) is from the removal of pump scatter.

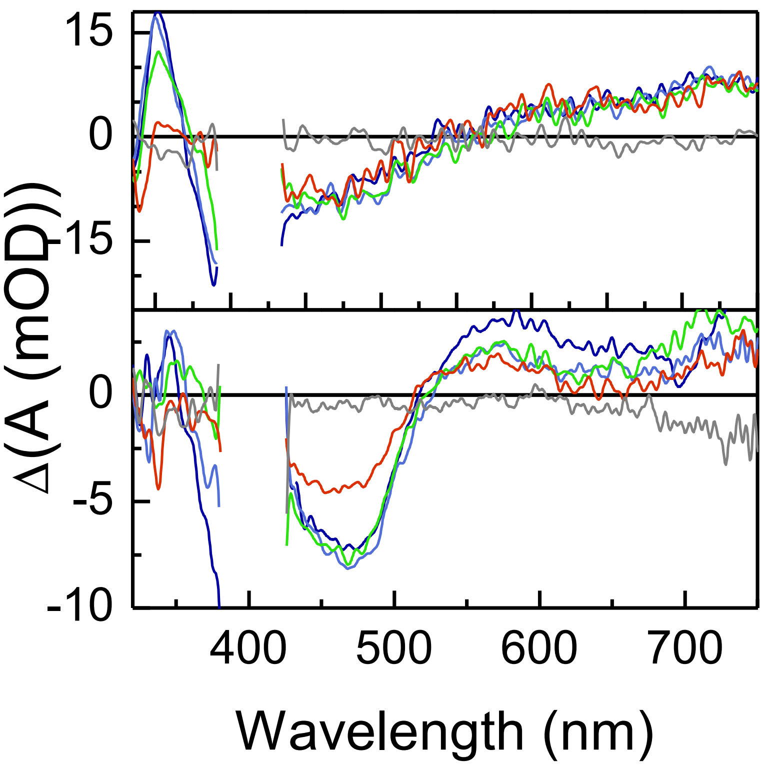

Figure S5: Spectral evolution and difference spectra during {$Ru^{II}(py)_4$} → {$Ru^{III}(py)_4$} oxidation process (initial: solid black curve, final: dashed red curve, intermediate: grey curves) of complexes **2** (left) and **3** (right) in DMSO (0.1 M [TBA]PF_6).

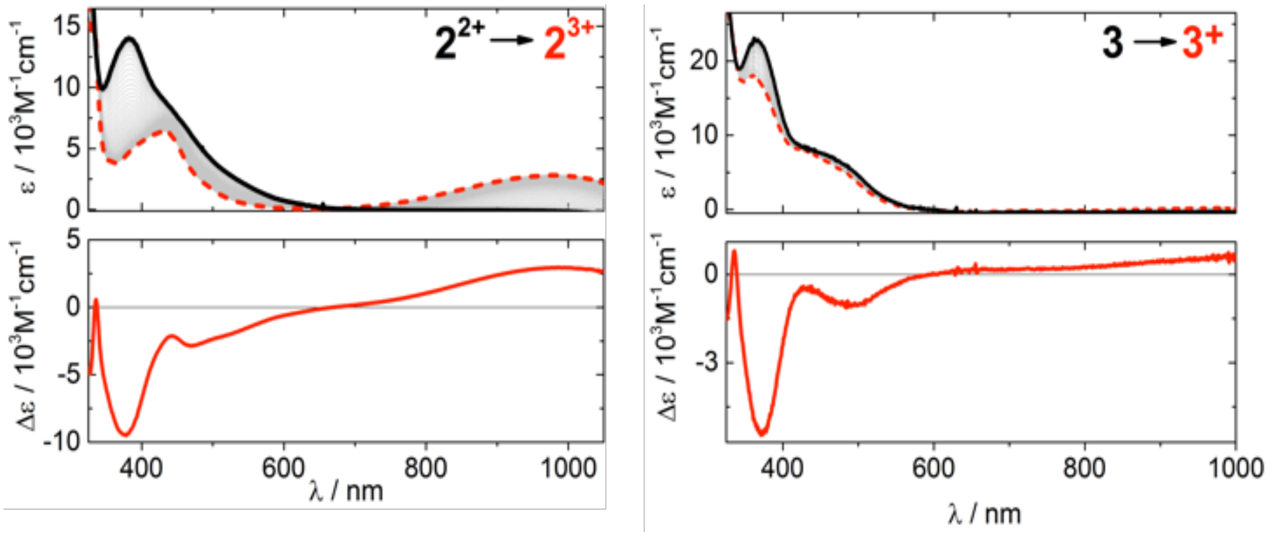

Figure S6: Spectral evolution and difference spectra during the tpy → tpy$^-$ reduction process (initial: solid black curve, final: dashed blue curve, intermediate: grey curves) of complexes of complexes **2** (left) and **3** (right) in DMSO (0.1 M [TBA]PF_6).

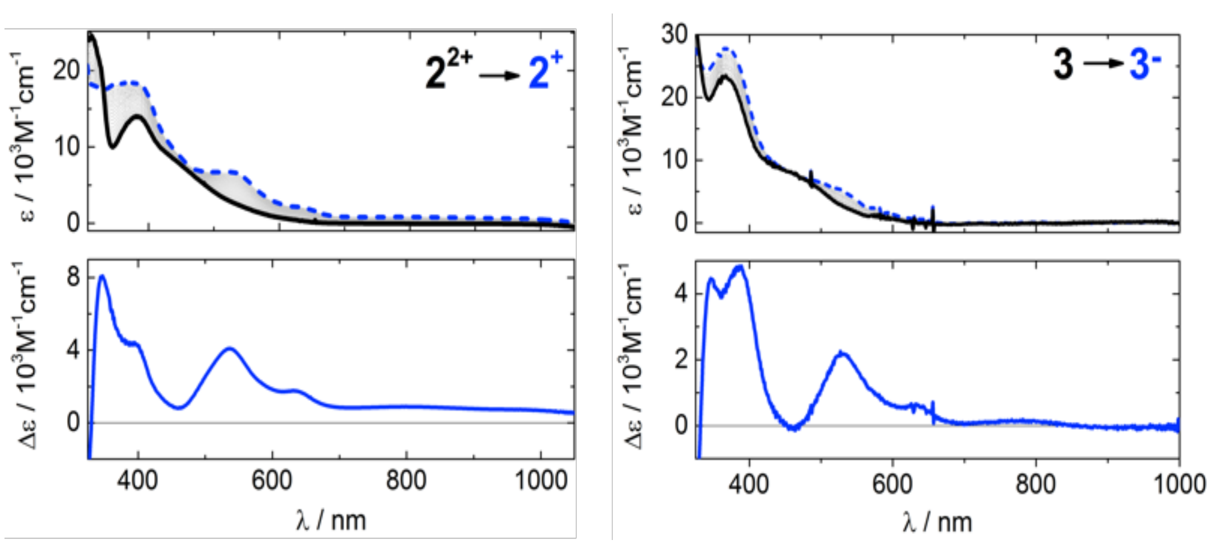

Figure S7: Sum of the oxidative and reductive difference spectra of complexes **2** and **3** in DMSO. Red and blue signals represent, respectively, the positive and negative expected signals in TA spectroscopy.

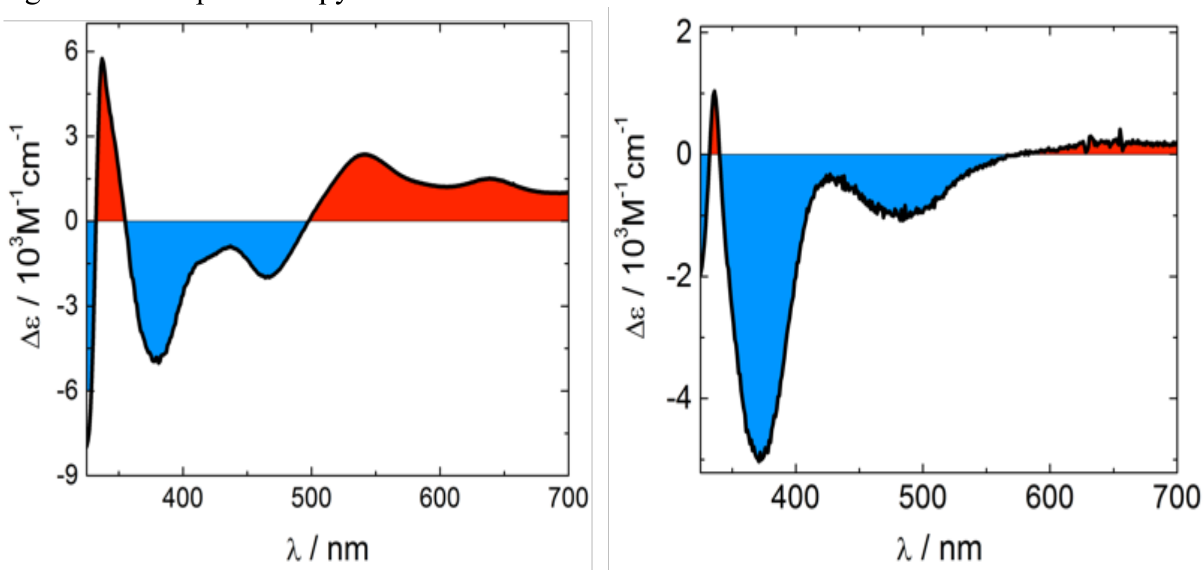

REFERENCES

1. Cadranel, A.; Albores, P.; Yamazaki, S.; Kleiman, V. D.; Baraldo, L. M., Efficient energy transfer via the cyanide bridge in dinuclear complexes containing Ru(II) polypyridine moieties. *Dalton Transactions* **2012,** *41* (17), 5343-5350.